Wind Energy Potentials and Its Trend in the South China Sea

Adekunle Ayodotun Osinowo[1], Xiaopei Lin[1], Dongliang Zhao[1] & Zhifeng Wang[2]

[1] College of Physical and Environmental Oceanography, Ocean University of China, China

[2] College of Engineering, Ocean University of China, Qingdao, China

Correspondence: Adekunle Ayodotun Osinowo, College of Physical and Environmental Oceanography, Ocean University of China, Qingdao, 266100, China. E-mails: voxfox99@yahoo.com; linxiaop@ouc.edu.cn; dlzhao@ouc.edu.cn; wzf1984@ouc.edu.cn

Abstract

Using a 30year (1976-2005) daily high-resolution reanalysis wind field dataset assimilated from several meteorological data sources, the wind speed and power characteristics of the South China Sea (SCS) were investigated using the Weibull shape and scale parameters. The region in general showed good wind characteristics. This is shown by high annual mean wind speed and power density values which are 5.93 m/s and 273.84 W/m^2 respectively.   The calculated annual mean wind power resource attributes the region to a relatively high potential site for large- scale grid connected wind turbine applications. The wind power ranged between 96.27 W/m^2 in May and 527.03 W/m^2 in December. Furthermore, spatio-temporal variations showed that strong trends in wind power exist in Luzon strait in the northern SCS and Xisha, Zhongsha, Luzon, Liyue bank in the central SCS which are evaluated as high wind potential regions and may be rated as locations excellent for installation of large wind turbines for electrical energy generation. Non-significant and negative trends dominate the southern SCS and may therefore, be suitable for small wind applications. The wind power density exhibited a significant increasing trend of 1.4 W/m^2 yr^{-1} in the SCS as a whole throughout the study period. The trend is strongest (2.8 W/m^2 yr^{-1}) in winter.

Keywords: potentials, region, trend, variation, weibull, wind power

1. Introduction

Energy is a key factor of life sustainability on earth in terms of human and economic development. The problems of poor energy distribution, adverse environmental effects of the several ways of energy production and declining fossil-fuel supplies are fast making life unbearable for people. With a rapid growing worldwide population, there is a large increase in the energy demand and there is the dire need for some new formulations to exploit renewable energy sources to generate power and electricity which the present and future generation will stand to benefit from. The wind resource is relevant in executing a wind energy project and an in-depth knowledge of the wind climate of a locality is a key requirement in the estimation of the performance of wind energy project. Among the sources of resource energy, the wind energy was the most rapid growing energy technology in terms of percentage of yearly growth of installed capacity per technology source (Lund ,2007), (Ackermann & Söder, 2002), (Akdag & Güler, 2010),   (Lund & Mathiesen, 2009).

With relatively little research and development expenditure, (Harborne & Hendry, 2009) found that wind has advanced more quickly to commercialization than other technologies such as solar power, fuel cells and wave power.

Talking about wind availability assessment, Nigeria was observed to be a poor/moderate wind regime with wind speeds within the range of 2.12 to 4.13 m/s in the southern part of Nigeria, except the coastal regions/offshore and the northern part where wind speeds were seen to range between 4.0 and 8.60 m/s   (Adaramola et al., 2014).

Encouragements have been shown for power applications regarding several researches carried out on wind speed assessment from many regions in the world. Recently, (Islam et al., 2011) carried out a research on the wind power characteristics and potentials for power generation at two locations in Malaysia with wind data observed at 10m hub height at the respective sites; they concluded that maximum monthly wind speeds of 4.8 and 4.3 m/s, and power density of 67.4 and 50.8 W/m^2 were found at Kudat and Labuan respectively. A similar study was also

carried out by (Mohammadi & Mostafaeipour, 2013) in assessing the possibility of wind energy for power application at a particular location in Kurdistan provinces on hourly, daily, monthly, seasonal and annual basis by using Weibull distribution function. The outcome of the study showed that the site is marginally suitable for wind power application.

Offshore wind energy is the energy generated by wind turbine set up in the sea. This area can be several tens of kilometres off the shoreline depending on the sea depth. Setting turbines in the sea has a tremendous advantage of better wind resources over that of land-based sites. Offshore turbines, therefore, achieve significantly more full-load hours. Offshore wind farms can be sited near large coastal demand centers, often avoiding long transmission lines to get power to demand, as can be the case for land-based renewable power installations – this makes offshore especially attractive for countries with coastal demand areas and land-based resources located far inland, such as the US, many European countries and China. In an attempt to satisfy environmental stakeholders, offshore wind farms generally face less public opposition and to date, less competition for space compared with developments on land. With this, projects can be large, with 1 GW power plants which is likely to be achievable in future.

Vast off shore deployment began at a very slow rate, particularly in Europe. As at the end of 2012, 5.4 GW had been installed (up from 1.5 GW in 2008) mainly in Denmark (1 GW) and the United Kingdom (3 GW) , with big offshore wind power plants installed in China, the Netherlands, Belgium, Germany and Sweden. More offshore turbines operate in Norway, Japan, Portugal and Korea, while new projects are planned in France and the United States. Forty six (46) GW of offshore projects are registered in the United Kingdom and about 10 GW have been progressing to consenting, construction or operation.

The wind energy, as it provides clean energy and a minimal-cost of energy sources, gives the best option of electricity generation of all renewable and non-renewable energy resources.

Wind energy generation in the SCS relies solely on suitable regions in the Sea for wind energy utilization, which varies with location and topography. Before a wind farm can be built, a thorough assessment of the wind energy potential in the SCS must be conducted. This can then be followed with detailed assessment in promising locations (Xydis et al., 2009). At present, there is very limited research on the assessment of wind energy potentiality in the SCS. Using a 30 year, reanalysis wind fields from various wind observations that were assimilated and provided every 6hour, this study therefore, aims at adopting the methodologies for wind energy assessment over land locations in previous studies to the Sea using the SCS as a case study. The spatial variations in wind power density which describes the choice of profitable region for harnessing wind energy together with the spatial trends in wind power, highlighting locations of strong trends in the SCS will be investigated and stand as an improvement on previous works. The temporal trends in wind power will also be analysed.

The paper is organized as follows. Section 2 provides information on the wind field data and a thorough validation of assimilated wind speed with wind speed obtained from altimeter using some statistical tests with their results.

Section 3 presents the methodologies used in the wind energy assessment and detailed discussion on results obtained. Finally, conclusions of this study are given in section 4.

2. Data Sets and Methodology

2.1 Wind Field Data

The simulation assimilated reanalysis wind fields from several wind observations were provided by South China Sea Institute of Oceanology, Chinese Academy of Sciences. The wind fields provided a 6hour time series of wind speed over a box extending from 3^0N to 23^0N and 105^0E to 121^0E which contains main part of SCS and surrounding waters and cover the period from 1976 to 2005.Wind fields were interpolated on a regular 0.25^0grid. With the use of the national centers for environmental prediction (NCEP) reanalysis data as the background wind field, sea surface wind field reanalysis used Grapes three-dimensional variation assimilation and weather research and forecasting (WRF) numerical model to simulate other meteorological data sourced from observed data, historical weather charts, NASA QuickSCAT data (0.25° resolution) and synoptic maps.

2.2 Satellite Data and Verification of Wind Field Assimilation

Usually, in-situ wind data are mainly collected from voluntary ships and wave buoys. However, in SCS, sparse voluntary ship data and no wave buoy data are available. This makes the remote sensing (use of satellite data) be an important source for the wind speed data in the SCS.
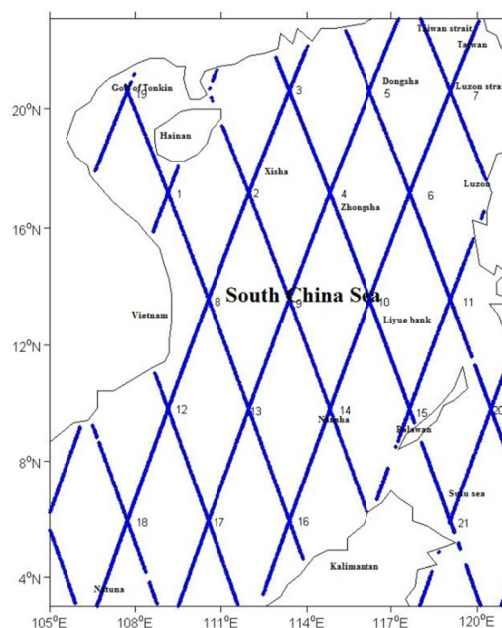
Figure 1. Topex/Poseidon crossover points and Geography of the SCS

The observation data used in this study were obtained from Topex/Poseidon (NASA/CNES) which is an official remote sensing data center that has data containing a near-real time gridded observations for significant wave height and wind speed. Topex/Poseidon was maneuvered into a 9.9156-day repeat period during which two Topex/Poseidon significant wave height and wind speed data are available at each crossover point.

The TOPEX/Poseidon wind speed data was used to verify the accuracy of the wind field assimilation. The TOPEX/Poseidon satellite crossover points in the SCS in 2002 are as shown in figure.1
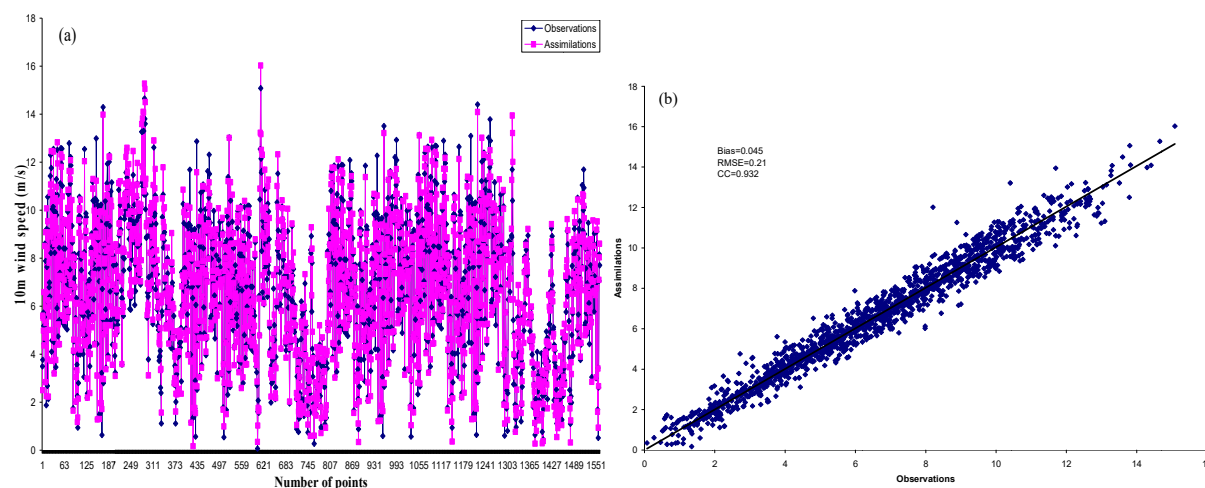
From 01-Jan-2002 to 31-Dec-2002

Figure 2. (a) Time series of assimilations against Topex/Poseidon data for the wind speed, on the x-axis is the number of data points. (b) Scatter plot of assimilation against Topex/Poseidon data for the wind speed

The assimilated wind speed data were interpolated into all the crossover points and comparisons were conducted between the assimilation and Topex/Poseidon altimeter observations. Synchronous comparisons of wind speeds are shown in figures 2a and 2b. The time series cover different periods in, 2002 for all the crossover points as

Topex/Poseidon passed over the SCS.

The accuracy of the wind field assimilation was evaluated through a conventional statistical analysis that consists on calculating the following:

$$cc = \frac{\sum_{i-1}^{n}(x_i - \bar{x})(y_i - \bar{y})}{\sqrt{\sum_{i-1}^{n}(x_i - \bar{x})^2 \sum_{i-1}^{n}(y_i - \bar{y})^2}} \tag{1}$$

$$Bias = \bar{y} - \bar{x} \tag{2}$$

$$RMSE = \sqrt{\frac{1}{N}\sum_{i-1}^{n}(y_i - x_i)^2} \tag{3}$$

Where, x_i represents the observed data, y_i represents the assimilated data, x and y are mean values of observed and assimilated data, N is the total number of observations.

The correlation coefficient (cc) between the assimilated and observed wind speed data is 0.932, the bias error is 0.045 m/s and a RMSE of 0.21 m/s.

In general, the assimilation results are consistent with the observations, which indicate that in general, wind field assimilation can reproduce the wind speed data in the SCS.

3. Analysis Methods

3.1 Computation of Wind Energy

For quite a long time, statistical models like Rayleigh, Weibull, log-normal and normal have been employed in wind data analysis (Fyrippis et al., 2010; Chang, 2011; Morgan et al., 2011; Keyhani et al., 2010; Lun & Lam, 2000) but the two-parameter Weibull probability distribution function had a world wide acceptability for wind data assessment because it has a good match with experimental data among the statistical models (Ohunakin et al., 2011). It is an overall gamma function that calculates the wind power density and describes the wind speed frequency distribution (Gokcek et al., 2007). This study therefore adopts the two-parameter weibull distribution function to compute the wind power density.

The Weibull probability density function is expressed as (Gokcek et al., 2007):

$$f(v) = \frac{k}{c}\left(\frac{v}{c}\right)^{k-1}\exp\left[-\left(\frac{v}{c}\right)^{k}\right] \tag{4}$$

The corresponding cumulative density function is expressed as (Gokcek et al., 2007):

$$F(v) = 1 - \exp\left[-\left(\frac{v}{c}\right)^{k}\right] \tag{5}$$

Where k and c are the shape and scale parameters respectively, while v is the wind speed. k is a dimensionless parameter which represents the variation of average wind speed in a given sample and c (m/s) is a variable which indicates the wind potential at a location and can be computed using approaches like standard deviation method (Justus et al., 1978), power density method (Akdag & Dinler, 2009), maximum likelihood method (Stevens & Smulders ,1979) and the graphical method (Rinne, 2010) etc. The stability of the wind speed is a function of 'k' the higher the value of 'k', the more stable the wind speed is. The larger the value of 'c' the more spread of wind power (Khan et al., 2015). This study therefore adopts the standard deviation method (Justus et al., 1978), (Saleh et al., 2012) in equations (6) and (7).

$$k = -\left(\frac{\sigma}{\bar{v}}\right)^{-1.086} \tag{6}$$

for $1 \leq k \leq 10$

$$c = \frac{\bar{v}}{\Gamma(1+1/k)} \tag{7}$$

$\bar{v}$ and σ are respectively the average wind speed in (m/s) and the standard deviation showing the extent of deviation of the wind speed. Γ(x) is the gamma function which is expressed as:

$$\Gamma(x) = \int_{0}^{\infty}\exp(-u)u^{x-1}dx \tag{8}$$

The wind power density is expressed as (Sathyajith, 2006):

$$p_d = \frac{1}{2}\rho c^3 \Gamma\left(1 + \frac{3}{k}\right) \tag{9}$$

Where P_d is the wind power density in W/m^2 and ρ is the air density assumed to be 1.225 kg/m^3.

The coefficient of variation (cov) which is the variability of wind speed, is the ratio between mean standard deviation to mean wind speed. The coefficient of variation (cov) is defined in percentage and can be expressed as (Ahmed, 2012):

$$COV\,(\%) = \frac{\sigma}{\overline{V}}\times 100 \tag{10}$$

In this study, wind speed data for the years 1976–2005 have been statistically analyzed. The monthly and seasonal variations of the Weibull parameters, wind power density, mean wind speed, standard deviation and cov are obtained. Furthermore, the spatial distribution of wind power density and its trends are analyzed.
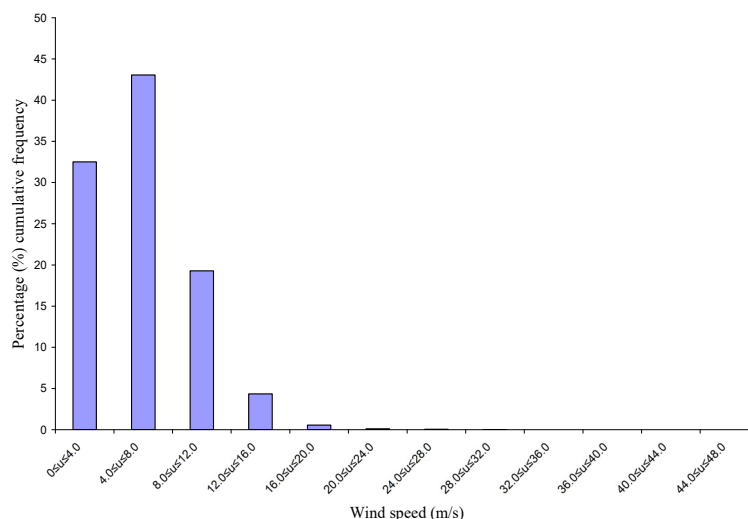
Figure 3. Percentage frequency distribution of wind speed in the SCS

3.2 Result and Discussion

3.2.1 Monthly Wind Pattern

Table 1. Monthly and annual mean wind speed parameters

Month	k	c (m/s)	WPD (W/m^2)	u (m/s)	σ	cov (%)
Jan	3.7	8.65	435.72	7.81	2.58	33.66
Feb	3.19	7.64	320.24	6.85	2.66	39.04
Mar	2.72	6.49	213.16	5.79	2.56	44.65
Apr	2.51	5.09	110.6	4.53	2.12	47.26
May	2.26	4.67	96.278	4.15	2.2	53.22
Jun	2.27	5.74	187.31	5.12	2.76	54.06
Jul	2.24	6.12	233.12	5.47	3.03	55.24
Aug	2.49	6.54	270.22	5.86	3.08	53.27
Sep	2.05	5.58	198.88	4.99	2.96	58.79
Oct	2.28	6.23	284.19	5.55	2.99	55.22
Nov	2.91	7.76	409.36	6.95	2.85	43.65
Dec	3.62	8.98	527.04	8.12	2.78	35.73
Annual	2.69	6.62	273.84	5.93	2.71	47.82

Note. k=Weibull shape parameter; c=Weibull scale parameter; WPD=Wind power density; u=10m wind speed; σ= Standard deviation; cov= coefficient of variation.
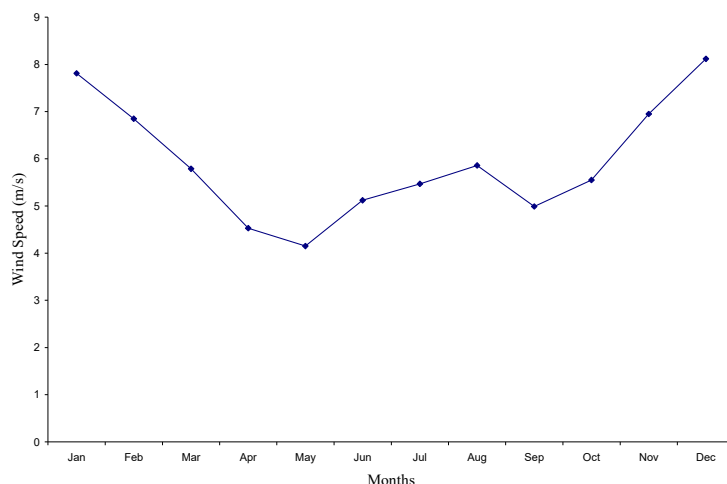
Figure 4. Monthly variation of 10m wind speed in the SCS

The percentage frequency distribution of wind speed in the SCS is illustrated in figure 3. The wind speed within the range of 4-8m/s has the highest frequency of 43.06%. The other wind speeds categories of 0-4m/s and 8-12m/s respectively have frequencies that differ by 13.2% while the wind speed in the range of 12-16m/s has a low frequency of 4.35%.

The monthly mean values of the Weibull parameters, wind power density, wind speed, standard deviation and coefficient of variation are listed in table 1. Figure.4 illustrates overall mean wind speed variations during different months in the SCS. The monthly mean wind speed varies between 4.15 m/s in May and 8.12 m/s in December. The monthly variations of the Weibull parameters are as shown in figure 5.
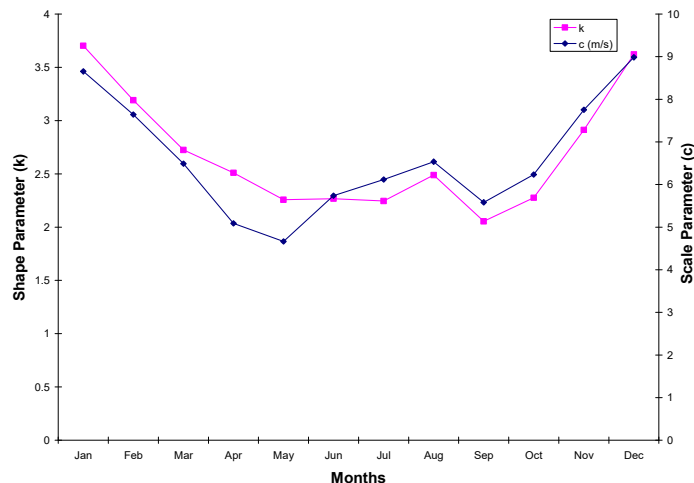
Figure 5. Monthly variation of the Weibull parameters in the SCS

The shape parameter 'k'varies between 2.05 in September and 3.7 in January which implies the wind speed data is most stable in January and least stable in September. Therefore, January is more suitable for the production of uninterrupted and stable wind power. The scale parameter 'c'ranges between 4.66 m/s in May and 8.98 m/s in December.

The minimum and maximum values of cov are between 33.66% in January and 58.78% in September. The highest value in September showed that the variation of wind speed is very high in September. The maximum and minimum values of standard deviation are equal to 3.07 and 2.11 obtained respectively in August and April.
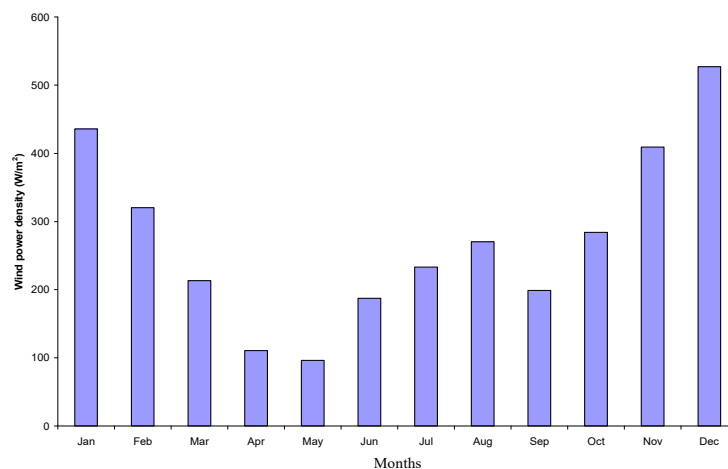
Figure 6. Monthly variation of wind power in the SCS

Table 2. Wind power classification: Elliot and Schwartz (1993)

Power Class	Power density (P (W/m^2)) at 10m
1	$0 < P \leq 100$
2	$100 < P \leq 150$
3	$150 < P \leq 200$
4	$200 < P \leq 250$
5	$250 < P \leq 300$
6	$300 < P \leq 400$
7	$400 < P \leq 1000$

Figure 6 displays the monthly variations of the wind power density in the SCS. Wind power density lies between 96.27 W/m^2 in May and 527.03 W/m^2 in December. The annual mean wind speed and wind power density stand at 5.93 m/s and 273.84 W/m^2 . For the wind power classification proposed by Elliot and Schwartz (1993) of Pacific Northwest Laboratory as shown in table 2, the annual mean power density for SCS falls into class 5 which means the classification places SCS as having relatively high potential for large-scale wind power applications.

3.2.2 Seasonal Wind Pattern

The months in each season in China can be classified as follows (1) Winter: December through February (2) Spring: March through May (3) Summer: June through August and (4) Autumn: September through November. The seasonal average values of wind speed are shown in figure 7.
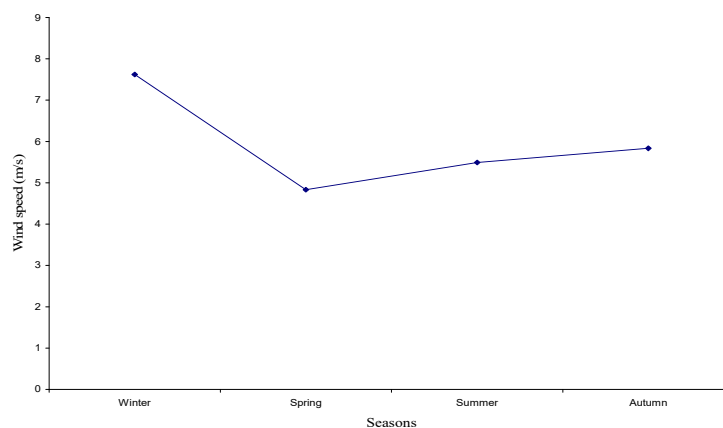

Figure 7. Seasonal variation of 10m wind speed in the SCS

Table 3. Seasonal mean wind speed parameters

Season	k	c (m/s)	WPD (W/m^2)	u (m/s)	σ	cov (%)
Winter	3.13	8.5	430.56	7.62	2.77	37.02
Spring	2.23	5.44	138.43	4.83	2.42	50.6
Summer	2.1	6.16	226.05	5.49	2.99	54.63
Autumn	2.04	6.57	294.55	5.83	3.13	54.04

Figure. 7 shows that the maximum value (7.62 m/s) occurred in winter and the minimum value (4.83 m/s) occurred in spring. Table 3 shows the seasonal averages of wind speed, standard deviation, cov, wind power density and Weibull parameters. From the table, the maximum and minimum values of the standard deviation occurred in autumn (3.12) and spring (2.42). The largest cov happened in summer (54.63%) and the smallest in winter (37.01%). The shape factor (k) ranged between 2.03 in autumn and 3.13 in winter. The scale factor (c) ranged between 5.43 m/s in spring and 8.5 m/s in winter.
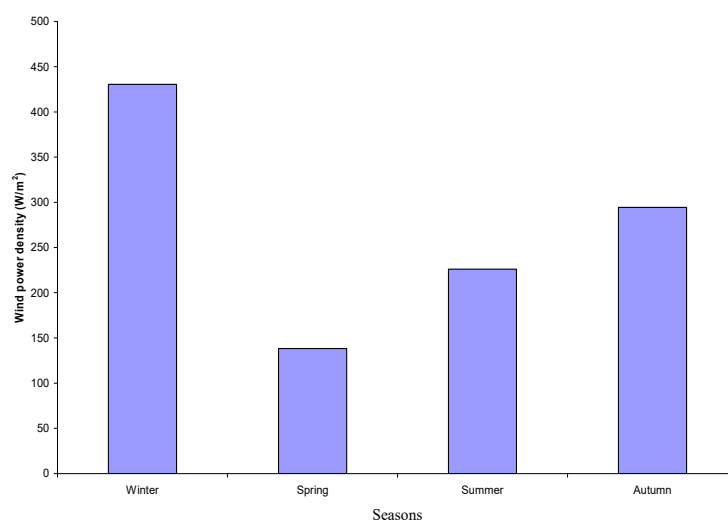

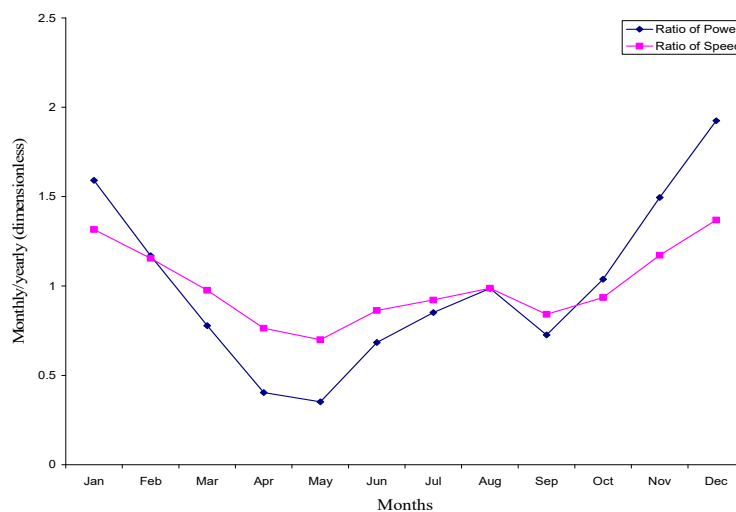Figure 8. Seasonal variation of wind power in the SCS

Figure 9. (Monthly/annual) ratio of mean wind power and mean wind speed in the SCS
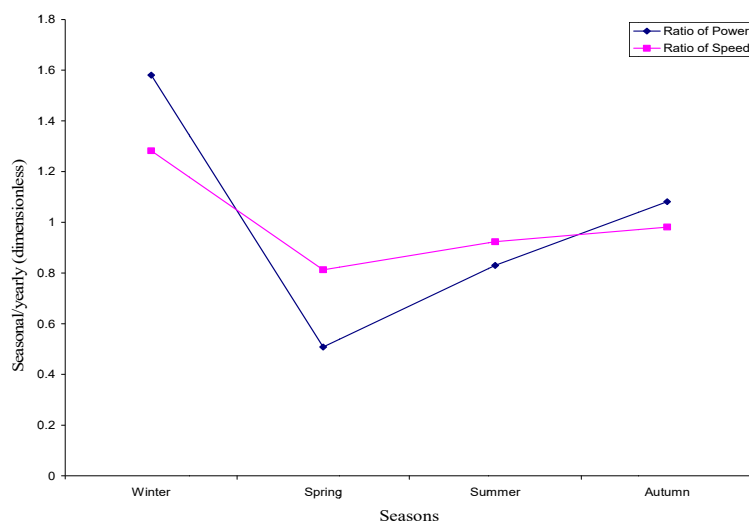
Figure 10. (Seasonal/annual) ratio of mean wind power and mean wind speed in the SCS

The seasonal variation of the wind power density is displayed in figure 8. Maximum wind power density (430.55 W/m^2) occurred in winter while minimum wind power density (138.42 W/m^2) occurred during spring.

Furthermore, dimensionless parameters to better understand the characteristics of wind in SCS are presented in figures 9 and 10. These are the ratios of monthly and seasonal mean wind speed and wind power density to the annual values of mean wind speed and wind power density.

The monthly to annual ratio of wind speed and wind power density presented in figure 9 shows that peak ratios of wind speed and wind power density occurred in December with ratios of 1.36 and 1.92 respectively. Minimum ratios of monthly to annual values of wind speed and wind power density occurred in May with ratios of 0.69 and 0.35 respectively. Also the seasonal to annual ratio of wind speed and wind power density shown in figure 10 depicts that peak ratios of wind speed and wind power density occurred in winter with ratios of 1.28 and 1.58 respectively while minimum ratios of seasonal to annual values of wind speed and wind power density occurred in spring with ratios of 0.81 and 0.5 respectively.

3.2.3 Spatial Distribution of Wind Power Density

This section describes the regional distribution of wind power density and identifies locations with high potential for wind power applications in the SCS.
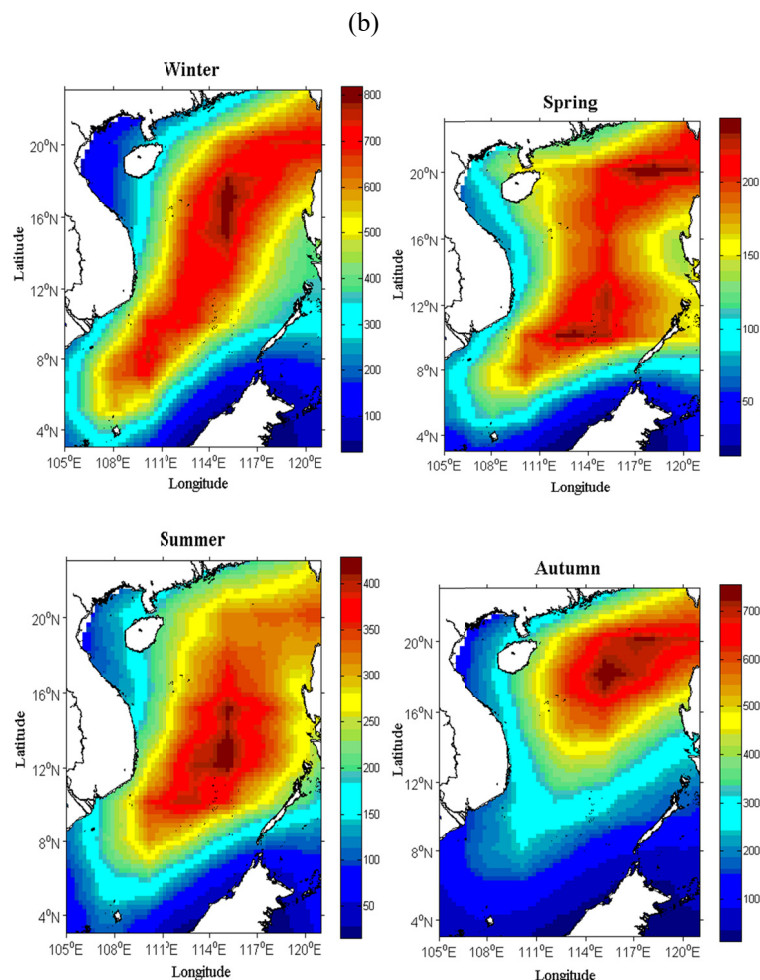
(a)

(b)
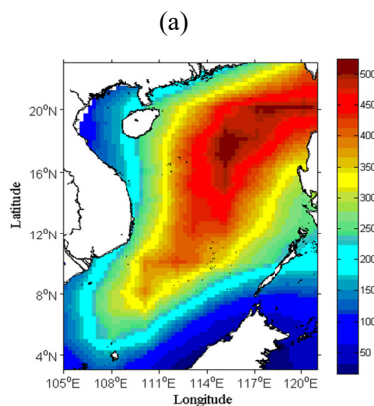
Figure 11. (a) annual and (b) seasonal distribution of wind power in the SCS. Values on the side bars are in W/m2

Figure 11a presents the annual mean distribution of wind power density in the SCS. The relative large area of high wind power distributes in the Luzon strait in the northern SCS and adjacent waters with values between 400 W/m^2 and 500 W/m^2. Locations such as Luzon strait and Zhongsha in the central SCS with largest values of wind power up to 520 W/m^2 exist in the high wind potential regions and have available potential for large wind turbine installation.

Regions particularly in the southern SCS and around Hainan and Tonkin Gulf in the northern SCS having wind power below 200 W/m^2 do not show good wind characteristics and this indicates that the regions may not be ideal for grid-connected electricity production but may have sufficient wind for small wind turbines.

The seasonal mean variation of the wind power in the SCS is shown in figure 11b. During winter, under the significant influence of the northeast trade wind caused by frequent and powerful cold air, the wind power is greater and occupies a larger region of the SCS as compared to other seasons. Wind power ranging between 600 W/m^2 and 800 W/m^2 distribute over a large part of the SCS and significant high values up to 800 W/m^2 are seen around Zhongsha.

During spring, the wind power is lowest in the whole year of smaller than 250 W/m^2 in most of the SCS. Relatively large area distribute in most part of the central and northern SCS with wind power being 170 W/m^2 - 250 W/m^2.

During summer, the wind power is slightly higher than in spring but smaller than 420 W/m^2 in most of the SCS. Relatively large area distribute in a large region of the central and northern SCS. The wind power is strongest, up to 420 W/m^2 around Zhongsha and Liyue bank in the central SCS.

During autumn, the wind power is clearly stronger than that in spring and summer. The relative large area

distributes in the Luzon strait and adjacent waters with wind power being 500 W/m^2 - 750 W/m^2. The wind power is strongest, up to 750 W/m^2 around Zhongsha and Luzon strait.

3.2.4 Spatial Trends in Wind Power Density

The regional variation of linear trends in wind power is described in this section and identifies locations with strong positive trends in the SCS.
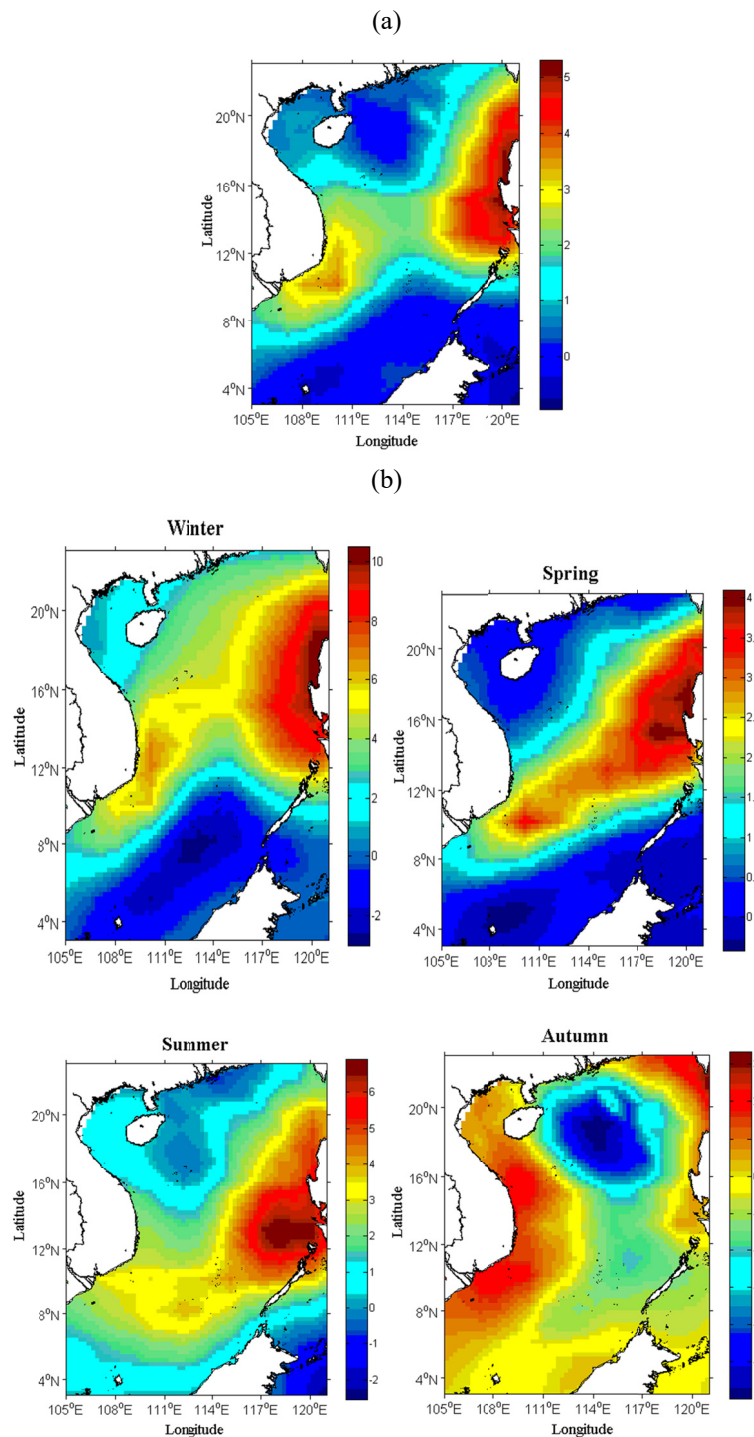
(a)

(b)

Figure 12. (a) annual and (b) seasonal trends of wind power in the SCS. Values on the side bars are in W/m2yr-1

The annual mean spatial trends in wind power are as shown in figure 12a. Non-significant trends distribute over most of the SCS. Large area of stronger trends 2 W/m^2yr^{-1} – 5 W/m^2yr^{-1} distribute over a large part of the central

and northern SCS. Increasing positive trends 3 W/m^2yr^{-1} – 5.2 W/m^2yr^{-1} are particularly seen in regions around Luzon strait down to Luzon and Liyue bank in the central SCS.

As shown in figure 12b, the long-term trend in wind power exhibits great seasonal differences. The area extent of the significant wind power increase is largest in winter, the area decreased in summer and spring and the smallest is in autumn.

In winter, most regions in the central and northern SCS showed a significant increase above 3 W/m^2yr^{-1}. Regions with relatively strong increase 8 W/m^2yr^{-1} – 10 W/m^2yr^{-1} are located around Luzon strait, Luzon and Liyue bank. The trends are non-significant and decreasing in every part of the southern SCS.

In spring, areas with significant increase 3 W/m^2yr^{-1} – 4 W/m^2yr^{-1} extend from Luzon strait to some few regions in the central SCS. Non-significant trends dominate the southern SCS and a large part of the northern SCS

In summer, regions with significant increase 3.5 W/m^2yr^{-1} – 7 W/m^2yr^{-1} also concentrate in Luzon strait, Luzon and Liyue bank. The trends are non-significant in most parts of the northern and southern SCS. Decreasing trends centre around Sulu sea and Borneo and some islands in the southern SCS.

In autumn, non-significant and decreasing trends distribute over most part of the SCS. Strong negative trends particularly centre around Dongsha island in the northern SCS and Xisha with Zhongsha in the central SCS. Only sporadic water bodies around Hainan island, Tonkin Gulf, Taiwan islands in the northern SCS and Vietnam borders in the central SCS showed slight increasing trends.

3.2.4 Temporal Trends in Wind Power Density

The overall annual variation of the SCS wind power density as shown in figure 13a is analyzed using linear regression method which passes the reliability test of 95%. The regression coefficient is 1.4 which means that the wind power density exhibits a significant increasing trend of 1.4 W/m^2yr^{-1} in the SCS as a whole throughout the 30 year period.
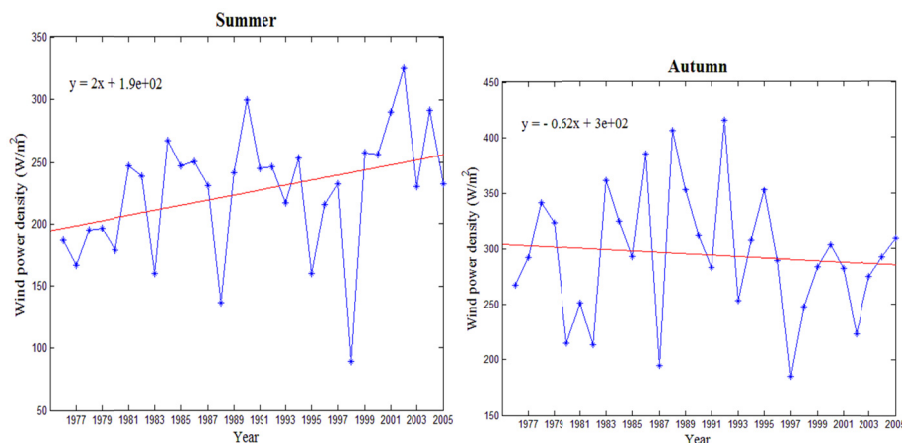
(a)

(b)
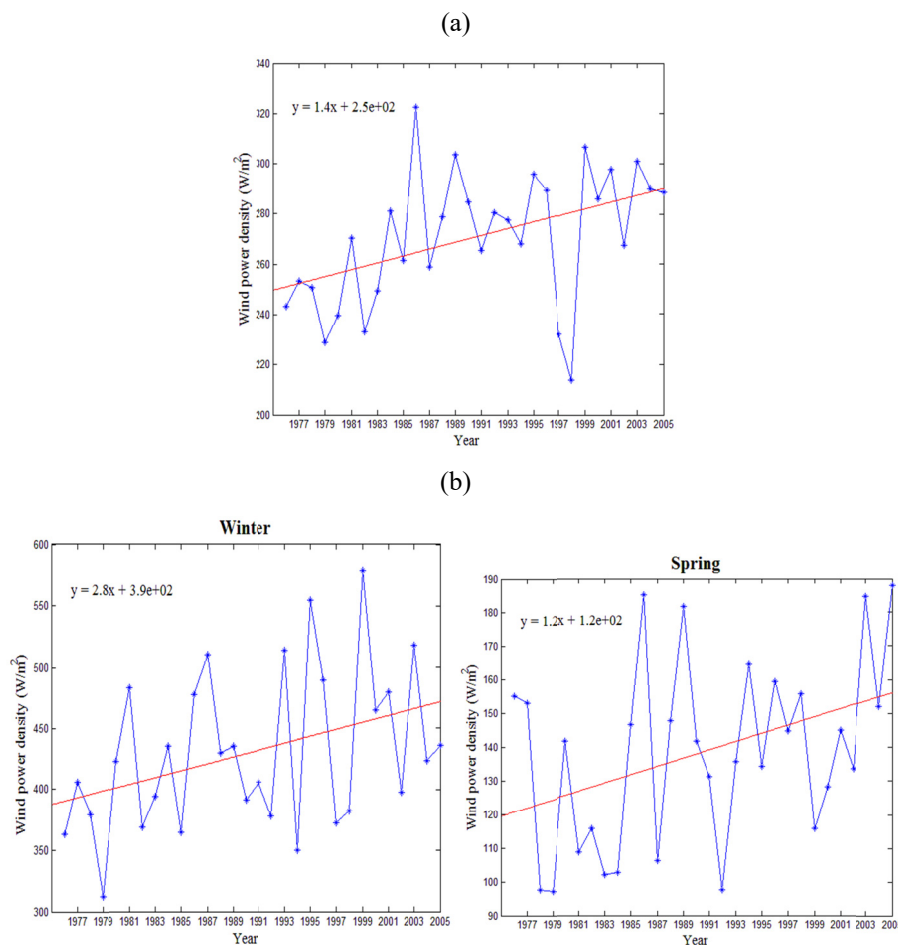
Figure 13. (a) annual and (b) seasonal variations of wind power in the SCS. Values on the side bars are in W/m2yr-1

Also presented in figure 13b are the overall seasonal variations of the wind power density in SCS. The SCS exhibited the most significant increase of 2.8 W/m2yr-1 during winter. This is followed by summer of 2 W/m2yr-1, spring of 1.2 W/m2yr-1 and a decreasing trend of -0.6 W/m2yr-1which occurred in autumn.

Table 4. 5 year trends of wind power for the year and seasons

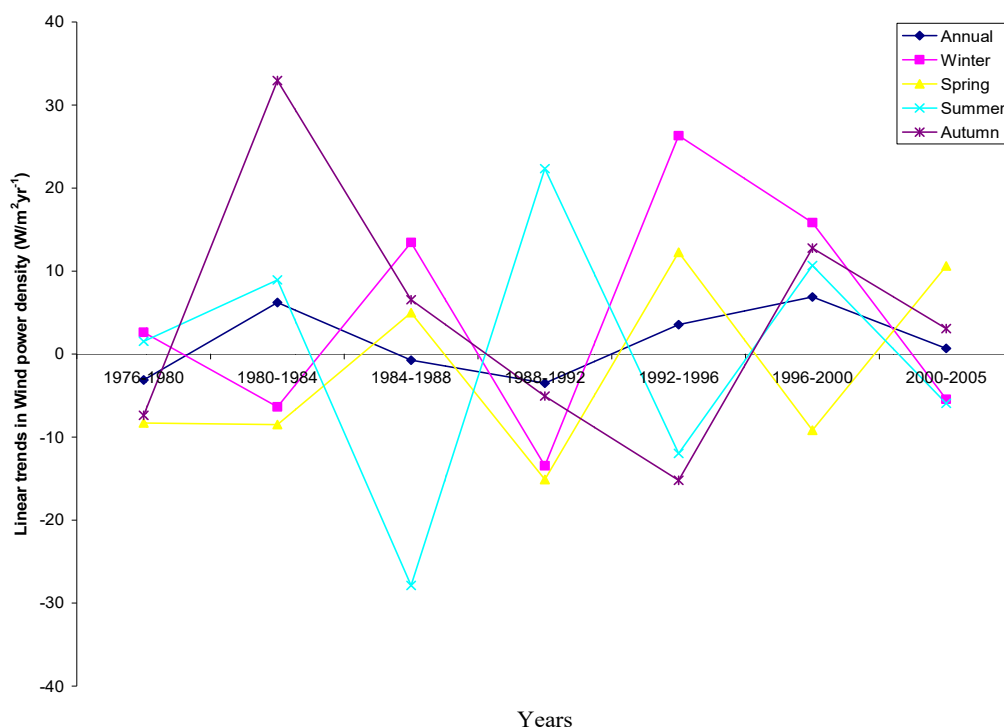| Year	Annual	Winter	Spring	Summer	Autumn
1976-1980	-3.12	2.62	-8.3	1.53	-7.37
1980-1984	6.21	-6.4	-8.48	8.94	32.96
1984-1988	-0.73	13.5	4.99	-28	6.54
1988-1992	-3.5	-13	-15.1	22.4	-5.06
1992-1996	3.55	26.3	12.27	-12	-15.19
1996-2000	6.87	15.8	-9.17	10.7	12.77
2000-2005	0.68	-5.4	10.62	-5.9	3.07

Figure 14. 5 year variation of wind power for the year and seasons

Table 4 further presents a 5year trends in wind power density for the whole year and seasons. The corresponding graphical plots are as shown in figure 14. Within the study period, the trend in wind power is strongest (6.87 W/m^2yr^{-1}) between years 1996 and 2000 while decreasing trends of -3.117 W/m^2yr^{-1}, -0.7314 W/m^2yr^{-1} and -3.49 W/m^2yr^{-1} are noticed between years 1976-1980, 1984-1988 and 1988-1992 respectively.

The strongest trend of 26.3 W/m^2yr^{-1} occurred between years 1992-1996 in winter. Negative trends of -6.37 W/m^2yr^{-1}, -13.38 W/m^2yr^{-1} and -5.42 W/m^2yr^{-1} occurred between years 1980-1984, 1988-1992 and 2000-2005 respectively.

During spring, the strongest trend of 12.27 W/m^2yr^{-1} is noticed between 1992 and 1996. Decreasing trends of -8.29 W/m^2yr^{-1}, -8.48 W/m^2yr^{-1}, -15.1 W/m^2yr^{-1} and -9.1 W/m^2yr^{-1} occurred between years 1976-1980, 1980-1984, 1988-1992 and 1996-2000.

In summer, the trend of 22.35 W/m^2yr^{-1} is strongest between years 1988-1992. Negative trends of -27.86 W/m^2yr^{-1}, -11.97 W/m^2yr^{-1} and -5.92 W/m^2yr^{-1} are noticed between years 1984-1988, 1992-1996 and 2000-2005 respectively.

Lastly in autumn, the highest trend of 32.96 W/m^2yr^{-1} occurred between years 1980-1984. Decreasing trends of -7.37 W/m^2yr^{-1}, -5.06 W/m^2yr^{-1} and -15.19 W/m^2yr^{-1} occurred in years 1976-1980, 1988-1992 and 1992-1996 respectively.

4. Conclusion

Over a 30year period (1976-2005), this study used a 6hourly, daily high-resolution reanalysis wind field dataset derived from some meteorological data sources to assess the spatio-temporal variation of the wind power potential using Weibull shape and scale parameters over the SCS. The major findings in the work are as follows:

(1) The region in general showed good wind characteristics. This is shown by high monthly and annual mean wind speed and power density values for the period of study

(2) The calculated annual mean wind power resource (273.84 W/m^2) attributes the region to a relatively high potential site for large- scale grid connected wind turbine applications

(3) The maximum wind speed of 8.12 m/s occurred in December and a minimum of 4.15 m/s occurred in May. The wind power ranged between 96.27 W/m^2 in May and 527.03 W/m^2 in December. The wind has the highest variation (58.78%) in September and the lowest (33.65%) in January

(4) The maximum wind speed of 7.62 m/s occurred in winter and the minimum of 4.83 m/s occurred in spring. The wind power ranged between 138.43 W/m^2 in spring and 430.55 W/m^2 in winter. The wind has the highest variation (54.63%) in summer and the lowest (37.01%) in winter

(5) The wind power is stronger in the central and northern SCS than in the southern SCS. Strongest wind power density exist around Luzon strait and its adjacent waters and may be rated as locations excellent for installation of large wind turbines for electrical energy generation

(6) Increasing positive trends in wind power density distribute in the Luzon strait and adjacent waters through Luzon to Liyue bank. Non-significant and negative trends dominate the southern SCS

(7) The wind power density exhibited a significant increasing trend of 1.4 $W/m^2 \ yr^{-1}$ in the SCS as a whole throughout the study period. The trend is strongest (2.8 $W/m^2 \ yr^{-1}$) in winter and weakest (-0.62 $W/m^2 \ yr^{-1}$) in autumn.

References

Ackermann, T., & Söder, L. (2002). An overview of wind energy-status 2002. *Renew Sustain Energ Rev, 6*(1), 67-127. http://dx.doi.org/10.1016/S1364-0321(02)00008-4

Adaramola, M. S., Oyewola, O. M., Ohunakin, O. S., & Akinnawonu, O. O. (2014). Performance evaluation of wind turbines for energy generation in Niger Delta, Nigeria", Sustainable Energy Technol Assess, 6, 75–85. http://dx.doi.org/10.1016/j.seta.2014.01.001

Ahmed, A. S. (2012). Potential wind power generation in South Egypt. *J. Renew Sustain Energy Rev, 16*(3), 1528–1536. http://dx.doi.org/10.1016/j.rser.2011.11.001

Akdag, S. A., & Dinler, A. (2009). A new method to estimate Weibull parameters for wind energy applications.

Energy Convers Manage, 50(7), 1761–1766. http://dx.doi.org/10.1016/j.enconman.2009.03.020

Akdag, S. A., & Güler, Ö. (2010). Evaluation of wind energy investment interest and electricity generation cost analysis for Turkey. *Appl Energ, 87*(8), 2574-80. http://dx.doi.org/10.1016/j.apenergy.2010.03.015

Chang, T. P. (2011). Estimation of wind energy potential using different probability density functions. *Appl Energy, 88*(5), 1848–1856. http://dx.doi.org/10.1016/j.apenergy.2010.11.010

Elliot, D., & Schwartz, M. (1993). Wind energy potential in the United States. Richland, WA: Pacific Northwest Laboratory PNL-SA-23109. NTIS no. DE94001667

Fyrippis, I., Axaopoulos, P. J., & Panayiotou, G. (2010). Wind energy potential assessment in Naxos Island, Greece. *Appl Energy, 87*(2), 577-586. http://dx.doi.org/10.1016/j.apenergy.2009.05.031

Gökçek, M., Bayülken, A., & Bekdemir, S. (2007). Investigation of wind characteristics and wind energy potential in Kirklareli, Turkey. *Renewable Energy, 32*(10), 1739-1752. http://dx.doi.org/10.1016/j.renene.2006.11.017

Harborne, P., & Hendry, C. (2009). Pathways to commercial wind power in the US, Europe and Japan: the role of demonstration projects and field trials in the innovation process. *Energ Policy, 37*(9), 3580-3595, http://dx.doi.org/10.1016/j.enpol.2009.04.027

Islam, M., Saidur, R., & Rahim, N. (2011). Assessment of wind energy potentiality at Kudat and Labuan, Malaysia using Weibull distribution function. *Energy, 36*(2), 985-92. http://dx.doi.org/10.1016/j.energy.2010.12.011

Justus, C., Hargraves, W., Mikhail, A., & Graber, D. (1978). Methods for estimating wind speed frequency distributions. *J. Appl Meteorol, 17*(3), 350-353. http://dx.doi.org/10.1175/1520-0450(1978)017<0350:MFEWSF>2.0.CO;2

Keyhani, A., Ghasemi,V. M., Khanali, M., & Abbaszadeh, R. (2010). An assessment of wind energy, potential as a power generation source in the capital of Iran, Tehran. *Energy, 35*(1), 188–201. http://dx.doi.org/10.1016/j.energy.2009.09.009

Khan, J. K., Ahmed, F., Uddin, Z., Iqbal, S. T., Saif, U. J., Siddiqui, A. A., & Aijaz, A. (2015). Determination of Weibull Parameter by four Numerical Methods and Prediction of Wind Speed in Jiwani (Balochistan). *J. Basic Appl Sci., 11*, 62-68. http://dx.doi.org/10.6000/1927-5129.2015.11.08

Lun, I. Y., & Lam, J. C. (2000). A study of Weibull parameters using long term wind observations. *Renewable Energ, 20*(2), 145–153. http://dx.doi.org/10.1016/S0960-1481(99)00103-2

Lund, H. (2007). Renewable energy strategies for sustainable development. *Energy, 32*(6), 912-919. http://dx.doi.org/10.1016/j.energy.2006.10.017

Lund, H., & Mathiesen, B. (2009). Energy system analysis of 100% renewable energy systems- the case of Denmark in years 2030 and 2050. *Energy, 34*(5), 524-531. http://dx.doi.org/10.1016/j.energy.2008.04.003

Mohammadi, K., & Mostafaeipour, A. (2013). Using different methods for comprehensive study of wind turbine utilization in Zarrineh, Iran. *Energy Convers Manage, 65*, 463-470. http://dx.doi.org/10.1016/j.enconman.2012.09.004

Morgan, E. C., Lackner, M., Vogel, R. M., & Baise, L. G. (2011). Probability distributions for offshore wind speeds", Energy Convers Manage, 52(1), 15–26. http://dx.doi.org/10.1016/j.enconman.2010.06.015

Ohunakin, O., Adaramola, M., & Oyewola, O. (2011). Wind energy evaluation for electricity generation using WECS in seven selected locations in Nigeria. *Appl Energy, 88*(9), 3197-3206. http://dx.doi.org/10.1016/j.apenergy.2011.03.022

Rinne, H. (2010). The Weibull distribution: a handbook. CRC Press.

Saleh, H., Abou El-Azm, A. A., & Abdel-Hady, S. (2012). Assessment of different methods used to estimate Weibull distribution parameters for wind speed in Zafarana wind farm, Suez Gulf, Egypt. *Energy, 44*(1), 710–719. http://dx.doi.org/10.1016/j.energy.2012.05.021

Sathyajith, M. (2006). Wind energy: fundamentals, resource analysis and economics", Springer Berlin Heidelberg. Print ISBN 978-3-540-30905-5. Online ISBN 978-3-540-30906-2. http://dx.doi.org/10.1007/3-540-30906-3

Stevens, M., & Smulders, P. (1979). The estimation of the parameters of the Weibull wind speed distribution for wind energy utilization purposes. *Wind Eng., 3*, 132-145.

Xydis, G., Koroneos, C., & Loizidou, M. (2009). Exergy analysis in a wind speed prognostic model as a wind farm sitting selection tool: a case study in Southern Greece. *Appl Energ, 86*(11), 2411-2420. http://dx.doi.org/10.1016/j.apenergy.2009.03.017

Copyrights